Chiral Solitons in Nuclei: Saturation, EMC Effect, and Drell-Yan Experiments

Jason R. Smith and Gerald A. Miller

Department of Physics, University of Washington, Seattle, Washington 98195-1560, USA

(Received 19 August 2003; published 20 November 2003)

The chiral quark-soliton model of the nucleon contains a mechanism for an attractive interaction between nucleons. This, along with the exchange of vector mesons between nucleons, is used to compute the saturation properties of infinite nuclear matter. This provides a new way to assess the effects of the nuclear medium on a nucleon that includes valence and sea quarks. We show that the model simultaneously describes the nuclear EMC effect and the related Drell-Yan experiments.

DOI: 10.1103/PhysRevLett.91.212301 PACS numbers: 25.30.Mr, 11.80.–m, 12.39.Fe, 13.60.–r

One frontier of strong interaction physics lies in the intermediate range of length scales available to present experiments where neither the fundamental theory, quantum chromodynamics (QCD), nor its low energy effective theory, chiral perturbation theory, have useful perturbative expansions. Neither fundamental quarks nor pointlike hadrons provide a complete description, so including the nonperturbative information that hadrons are bound states of valence quarks in a polarized vacuum is necessary. One way to probe these intermediate length scales and this nonperturbative physics is to examine the short distance structure of a large object. The prime example is the European Muon Collaboration (EMC) effect [1] where the short distance (~ 5 GeV or $\sim 10^{-2}$ fm) structure of nuclei differs from that of a collection of free nucleons. This measurement showed that bound nucleons are different than free ones and implied that the medium modifications could be significant for any nuclear observable [2]. Indeed, a recent paper [3] obtains evidence for a medium modification of the elastic proton form factor.

Our central concern is the depletion of the nuclear structure function $F_2^A(x)$ in the valence quark regime $0.3 \lesssim x \lesssim 0.8$. While the general interpretation is that a valence quark in a bound nucleon has less momentum than in a free one, corresponding to some increased length scale, the specific mechanism for this has eluded a universally accepted explanation for 20 years [2,4–6]. A popular explanation is the so-called "binding" effect which originates from a possible mechanism in which mesons binding the nucleus carry momentum. An important consequence is that the mesonic presence would enhance the antiquark content of the nucleus [7,8]. Such an effect has not been seen in Drell-Yan experiments [9] in which a quark in a proton beam annihilates with an antiquark in a nuclear target producing a muon pair. Furthermore, relativistic treatments, including the light-cone approach needed to obtain the nucleon structure function, of the binding effect with structureless hadrons fail [10–13], suggesting that modifications of the internal quark structure of the nucleon are required to explain the deep inelastic scattering data.

Any description of the EMC effect must be consistent with the constraints set by both deep inelastic scattering and Drell-Yan data. Thus a successful model must include antiquarks as well as quarks and show how the medium modifies both the valence and sea quark distributions. Our purpose is to provide a mechanism for that modification within the chiral quark-soliton (CQS) model [14–17]. This phenomenological model has many desirable qualities: the ability to describe a wide class of hadron observables with surprising accuracy, the inclusion of antiquarks, positivity of generalized parton distributions, and a basis in QCD [16]. The model also predicted [18] the recently discovered θ^+ exotic baryon resonance [19,20]. Here we show how the model describes nuclear saturation properties, reproduces the EMC effect, and satisfies the bounds on nuclear antiquark enhancement provided by Drell-Yan experiments.

The CQS model Lagrangian with (anti)quark fields $\overline{\psi}, \psi$ and profile function $\Theta(r)$ is

$$\mathcal{L} = \overline{\psi}(i\partial\!\!\!/ - Me^{i\gamma_5 \boldsymbol{n}\cdot\boldsymbol{\tau}\Theta(r)})\psi, \tag{1}$$

where $\Theta(r \to \infty) = 0$ and $\Theta(0) = -\pi$ to produce a soliton with unit winding number. The quark spectrum consists of a single bound state and a filled negative energy Dirac continuum; the vacuum is the filled negative continuum with $\Theta = 0$. The wave functions in this spectrum provide the input for the quark and antiquark distributions used to calculate the nucleon structure function.

We work to leading order in the number of colors ($N_C = 3$), with $N_f = 2$, and in the chiral limit. While the former characterizes the primary source of theoretical error, one could systematically expand in N_C to calculate corrections. We take the constituent quark mass to be $M = 420$ MeV, which reproduces, for example, the N-Δ mass splitting at higher order in the N_C expansion and other observables [17].

The theory contains divergences that must be regulated. We use a single Pauli-Villars subtraction as in Ref. [21] because we follow that work to calculate the quark distribution functions. The Pauli-Villars mass is determined

by reproducing the measured value of the pion decay constant, $f_\pi = 93$ MeV, with the relevant divergent loop integral regularized using $M_{\rm PV} \simeq 580$ MeV. This regularization also preserves the completeness of the quark states [21].

The nucleon mass is given by a sum of the energy of a single valence level (E^v), and the regulated energy of the soliton (E_Θ, equal to the energy in the negative Dirac continuum with the energy in the vacuum subtracted)

$$M_N = N_C E^v + E_\Theta(M) - \frac{M^2}{M_{\rm PV}^2} E_\Theta(M_{\rm PV}). \tag{2}$$

The field equation for the profile function is

$$\Theta(r) = \arctan\frac{\rho_{ps}^q(r)}{\rho_s^q(r)}, \tag{3}$$

where ρ_s^q and ρ_{ps}^q are the quark scalar and pseudoscalar densities, respectively.

The dependence of nucleon properties on the nuclear medium is incorporated in the model by simply letting the quark scalar density in the field equation (3) contain a (constant) contribution arising from other nucleons present in symmetric nuclear matter. This models a scalar interaction via the exchange of multiple pairs of pions between nucleons. We take the scalar density to consist of three terms: (1) the constant condensate value $\langle\overline{\psi}\psi\rangle_0$ (in the vacuum or at large distances from a free nucleon), (2) the valence contribution ρ_s^v, and (3) the contribution from the medium which takes the form of the convolution of the nucleon ρ_s^N and valence quark scalar densities as in the quark-meson coupling (QMC) model [22–24]

$$\rho_s^q(r) \simeq \langle\overline{\psi}\psi\rangle_0 + \rho_s^v(r) + \int d^3r' \rho_s^N(r')\rho_s^v(r - r'). \tag{4}$$

We take the pseudoscalar density to have only the valence term $\rho_{ps}^q \simeq \rho_{ps}^v$; the two other contributions analogous to the first and third terms of Eq. (4) vanish due to symmetries of the QCD vacuum and nuclear matter. These approximations to the densities neglect the precise form of the negative continuum wave functions in Eq. (3). The resulting free nucleon profile function has no discernible difference from a fully self-consistent treatment, demonstrating the excellence of this approximation.

We take the vacuum value of the chiral condensate in Eq. (4) to be a free parameter, but in the single Pauli-Villars regularization, the scalar and pseudoscalar densities contain a divergence that cancels in the ratio Eq. (3) [25]. A finite value of the ratio is obtained by normalizing the densities so that the cancellation occurs (by dividing the other terms in the numerator and denominator by the same divergent quantity). This yields a free nucleon mass that is independent of $\langle\overline{\psi}\psi\rangle_0$ (as is necessary because it is divergent in single Pauli-Villars regularization) and a medium contribution that enters only through the ratio $\rho_s^N/\langle\overline{\psi}\psi\rangle_0$. While the vacuum value of the condensate does not vary by definition, the effective condensate $\langle\overline{\psi}\psi\rangle_0 + \rho_s^N S(k_F)$, where $S(k_F)$ is an integral of ρ_s^v [see Eq. (4)], falls $\sim$30% at nuclear density. This is consistent with the model independent result [26] that predicts a value 25%–50% below the vacuum value.

The nucleon scalar density is determined by solving the nuclear self-consistency equation

$$\rho_s^N = 4\int^{k_F} \frac{d^3k}{(2\pi)^3} \frac{M_N(\rho_s^N)}{\sqrt{k^2 + M_N(\rho_s^N)^2}}. \tag{5}$$

The dependence of the nucleon mass, and any other properties calculable in the model, on the Fermi momentum k_F enters through Eq. (5). Thus there are two coupled self-consistency equations: one for the profile, Eq. (3), and one for the density, Eq. (5). These are iterated until the change in the nucleon mass Eq. (2) is as small as desired for each value of the Fermi momentum. We use the Kahana-Ripka (KR) basis [27], with momentum cutoff and box size extrapolated to infinity, to evaluate the energy eigenvalues and wave functions used as input for the densities, nucleon mass, and quark distributions.

A phenomenological vector meson (mass $m_v = 770$ MeV) exchanged between nucleons (but not quarks in the same nucleon) is introduced [28] to obtain the necessary short distance repulsion which stabilizes the nucleus. The resulting energy per nucleon is

$$\frac{E}{A} = \frac{4}{\rho_B(k_F)}\int^{k_F} \frac{d^3k}{(2\pi)^3}\sqrt{k^2 + M_N(k_F)^2} + \frac{1}{2}\frac{g_v^2}{m_v^2}\rho_B(k_F). \tag{6}$$

We now present the results. The mass of a free nucleon is computed to be $M_N(k_F = 0) = 1209$ MeV. The $\sim$30% difference is as expected in the model at leading order in N_C. We evaluate the nucleon mass Eq. (2) and energy per nucleon Eq. (6) as a function of k_F for three values of the condensate. We plot $B = E/A - M_N(0)$ in Fig. 1 where we

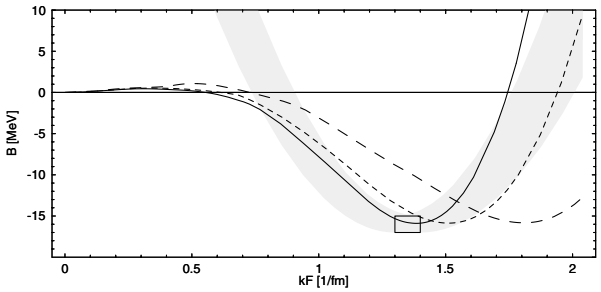

FIG. 1. Binding energy per nucleon as a function of Fermi momentum fit to $B = -15.75$ MeV at the minimum for $\langle\overline{\psi}\psi\rangle_0 = -(225\ \text{MeV})^3$ (long-dashed line), $-(210\ \text{MeV})^3$ (short-dashed line), and $-(200\ \text{MeV})^3$ (solid line). The box and shaded region are the experimental uncertainty [29] in the binding energy, density, and compressibility of nuclear matter.

choose the vector meson coupling to fit $B = -15.75$ MeV at the minimum.

We use the value $-\langle\bar{\psi}\psi\rangle_0^{1/3} = 200$ MeV, and vector coupling $g_v^2/4\pi = 10.55$, which gives a Fermi momentum of $k_F = 1.38$ fm^{-1} in nuclear matter consistent with the known value $k_F = 1.35 \pm 0.05$ fm^{-1} [29]. The compressibility is $K = 348.5$ MeV which is above the experimental value $K = 210 \pm 30$ MeV, but well below the Walecka model value of 560 MeV.

The isoscalar unpolarized distribution $q(x) = u(x) + d(x)$ is the leading order term in N_C, with the isovector unpolarized quark distribution $u(x) - d(x)$ smaller by a factor $\sim 1/N_c$ and set to zero. The distributions are calculated using the KR basis at $k_F = 0$ and $k_F = 1.38$ fm^{-1} almost exactly as in Ref. [21] where the quark distribution is given by the matrix element

$$q(x) = N_C M_N \sum_n \langle\psi_n|(1 + \gamma^0\gamma^3)\delta(E_n + p^3 - xM_N)|\psi_n\rangle, \tag{7}$$

with the regulated sum taken over occupied states. The eigenvalues E_n are determined from diagonalizing the Hamiltonian, derived from the Lagrangian (1), in the KR basis. The vector meson exchange is not explicit in Eq. (7) because the initial, intermediate, and final states of the struck and spectator quarks experience the same vector potential, as demanded by consistency. Thus we include the interaction of the debris of the struck nucleon with the residual nucleus [23]. The antiquark distribution is given by $\bar{q}(x) = -q(-x)$ where the sum is over unoccupied states. We use the exact sea wave functions, and not the approximation used in Eq. (4). The use of a finite basis causes the distributions to be discontinuous. These distributions are smooth functions of x in the limit of infinite momentum cutoff and box size, but numerical calculations are made at finite values and leave some residual roughness. This is overcome in Ref. [21] by introducing a smoothing function. We deviate from their procedure and do not smooth the results; instead we find the subsequent one-loop perturbative QCD evolution [30] to be sufficient.

These distributions are used as input at a scale of $Q = M_{\rm PV} \simeq 580$ MeV for evolution to $Q = 5$ GeV in the case of the quark singlet distribution $q^S(x) = q(x) + \bar{q}(x) \propto F_2^N(x)/x$ at leading order in N_C. The EMC ratio function is defined to be

$$R(x, Q^2) = \frac{F_2^A(x, Q^2, k_F)}{AF_2^N(x, Q^2, k_F = 0)}, \tag{8}$$

$$F_2^A(x, Q^2, k_F) = \int_x^A dy f(y) F_2^N(x/y, Q^2, k_F).$$

The nucleon momentum distribution, following from a light-cone approach, for any mean field theory of nuclear matter [10] is

$$f(y) = \frac{3}{4\Delta_F^3}\theta(1 + \Delta_F - y)\theta(y - 1 + \Delta_F)[\Delta_F^2 - (1 - y)^2], \tag{9}$$

where $\Delta_F = k_F/\overline{M}_N$ and $\overline{M}_N = M_N(0) - 15.75$ MeV. The antiquark distribution $\bar{q}(x)$ is evolved to $Q = 10$ GeV for use in the Drell-Yan ratio $\bar{q}^A/A\bar{q}$, analogous to Eq. (8). The EMC and Drell-Yan ratios are plotted in Fig. 2. While the data shown in Fig. 2 are for large, but finite, nuclei, our calculation reproduces the trend of both sets of data. It falls slightly below the SLAC-E139 data [31] due to the higher density of nuclear matter.

In Fig. 3 we show the quark, antiquark, singlet, and valence ($q^v = q - \bar{q}$) quark distributions weighted by x for a free and bound nucleon at a scale $Q = 5$ GeV. There is a large depletion in the bound nucleon valence distribution in Fig. 3, that, if used to calculate the EMC ratio (8), produces too large an effect. This large effect is comparable to that of the QMC model impulse approximation calculation or the Guichon model [23] which include only valence quarks. This valence effect is mitigated by a small enhancement in $x\bar{q}$, consistent with the Drell-Yan data, so that the singlet distribution has only a moderate depletion consistent with the EMC effect.

A simple picture in terms of the uncertainty principle is available. The influence of the nuclear medium on the nucleon causes the root mean square radius of the baryon density to increase by 2.4%. This corresponds to a decreased momentum and a depletion of the bound structure function relative to the free one. This swelling is consistent with a $<6\%$ increase as constrained by quasielastic

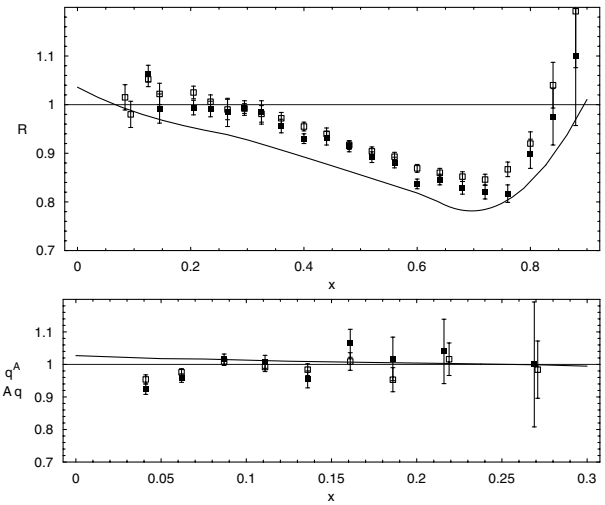

FIG. 2. The EMC (top panel) and the Drell-Yan (bottom panel) ratios at scales $Q = 5$ GeV and 10 GeV, respectively, for nuclear matter. The data are for iron (empty boxes) and gold (filled boxes) from SLAC-E139 (top panel) [31], for iron (empty boxes) and tungsten (filled boxes) from FNAL-E772 (bottom panel) [9].

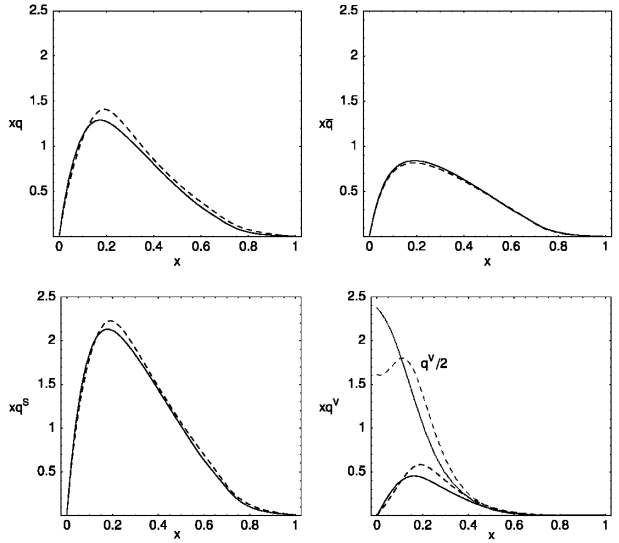

FIG. 3. Clockwise from top left the distributions $xq(x)$, $x\bar{q}(x)$, $xq^V(x)$, and $xq^S(x)$ in a free (dashed lines) and bound (solid lines) nucleon at a scale $Q = 5$ GeV. The valence distribution $q^V(x)/2$ is also shown in gray in the lower right graph.

inclusive electron-nucleus scattering data [32] and the recent polarization transfer measurement [3].

We ignore the effects of shadowing, which occur when the virtual photon striking the nucleus fluctuates into a quark-antiquark pair over a distance $\sim 1/2M_N x$ exceeding the internucleon separation. This causes a depletion in the structure function for $x \lesssim 0.1$ and is relatively well understood [2,4–6] and so we do not reiterate those results. Additionally, we ignore contributions from quantum pion structure functions, which in this model propagate through constituent quark loops, and would modify the behavior at small x. These loops are suppressed by $\mathcal{O}(1/N_C)$ and are not treated at leading order.

The present model provides a intuitive, qualitative treatment that maintains consistency with all of the free nucleon properties calculated by others [16,17]. It gives a reasonable description of nuclear saturation properties, reproduces the EMC effect, and satisfies the constraints on the nuclear sea obtained from Drell-Yan experiments with only two free parameters: $\langle\bar{\psi}\psi\rangle_0$ and g_v.

The central mechanism to explain the EMC effect is that the nuclear medium provides an attractive scalar interaction that modifies the nucleon wave function. This is also the dominant mechanism in the QMC model approach to the EMC effect [23] and also similar to the quark delocalization approach [33]. The improvements given here are the explicit computation of the effects of the medium on the antiquark distributions so that consistency with the Drell-Yan data could be verified and the reduction of the number of input parameters and model assumptions. Our extension of the chiral quark-soliton model to nuclear matter provides a new, consistent way to calculate possible medium modifications of a variety of observables that could be measured in experiments.

We would like to thank the USDOE for partial support of this work and S. D. Ellis for useful comments.

[1] J. J. Aubert *et al.*, Phys. Lett. **123B**, 275 (1983).
[2] D. F. Geesaman, K. Saito, and A. W. Thomas, Annu. Rev. Nucl. Part. Sci. **45**, 337 (1995).
[3] S. Strauch *et al.*, Phys. Rev. Lett. **91**, 052301 (2003).
[4] G. Piller and W. Weise, Phys. Rep. **330**, 1 (2000).
[5] M. Arneodo, Phys. Rep. **240**, 301 (1994).
[6] M. M. Sargsian *et al.*, J. Phys. G **29**, R1 (2003).
[7] R. P. Bickerstaff, M. C. Birse, and G. A. Miller, Phys. Rev. Lett. **53**, 2532 (1984).
[8] M. Ericson and A. W. Thomas, Phys. Lett. **148B**, 191 (1984).
[9] D. M. Alde *et al.*, Phys. Rev. Lett. **64**, 2479 (1990).
[10] G. A. Miller and J. R. Smith, Phys. Rev. C **65**, 015211 (2002).
[11] J. R. Smith and G. A. Miller, Phys. Rev. C **65**, 055206 (2002).
[12] M. C. Birse, Phys. Lett. B **299**, 186 (1993).
[13] L. L. Frankfurt and M. I. Strikman, Phys. Lett. B **183**, 254 (1987).
[14] S. Kahana, G. Ripka, and V. Soni, Nucl. Phys. **A415**, 351 (1984).
[15] M. C. Birse and M. K. Banerjee, Phys. Lett. **136B**, 284 (1984).
[16] D. Diakonov and V. Y. Petrov, hep-ph/0009006.
[17] C. V. Christov *et al.*, Prog. Part. Nucl. Phys. **37**, 91 (1996).
[18] D. Diakonov, V. Petrov, and M. V. Polyakov, Z. Phys. A **359**, 305 (1997).
[19] V. V. Barmin *et al.*, hep-ex/0304040.
[20] T. Nakano *et al.*, hep-ex/0301020.
[21] D. Diakonov *et al.*, Phys. Rev. D **56**, 4069 (1997).
[22] K. Saito and A. W. Thomas, Phys. Lett. B **327**, 9 (1994).
[23] K. Saito and A. W. Thomas, Nucl. Phys. **A574**, 659 (1994).
[24] P. G. Blunden and G. A. Miller, Phys. Rev. C **54**, 359 (1996).
[25] T. Kubota, M. Wakamatsu, and T. Watabe, Phys. Rev. D **60**, 014016 (1999).
[26] T. D. Cohen, R. J. Furnstahl, and D. K. Griegel, Phys. Rev. C **45**, 1881 (1992).
[27] S. Kahana and G. Ripka, Nucl. Phys. **A429**, 462 (1984).
[28] J. D. Walecka, Ann. Phys. (N.Y.) **83**, 491 (1974).
[29] J. P. Blaizot, Phys. Rep. **64**, 171 (1980).
[30] K. Hagiwara *et al.*, Phys. Rev. D **66**, 010001 (2002).
[31] J. Gomez *et al.*, Phys. Rev. D **49**, 4348 (1994).
[32] R. D. Mckeown, Phys. Rev. Lett. **56**, 1452 (1986).
[33] C. J. Benesh, T. Goldman, and G. J. Stephenson, nucl-th/0307038.